Langmuir

ARTICLE

pubs.acs.org/Langmuir

Thermodynamic and Structural Characterization of Zwitterionic Micelles of the Membrane Protein Solubilizing Amidosulfobetaine Surfactants ASB-14 and ASB-16

Mariana G. D'Andrea,[†,‡] Cleyton C. Domingues,[§,‡] Sonia V. P. Malheiros,[∥] Francisco Gomes Neto,[⊥] Leandro R. S. Barbosa,[○] Rosangela Itri,[○] Fabio C. L. Almeida,[⊥] Eneida de Paula,[§] and M. Lucia Bianconi[†,*]

[†]Laboratório de Biocalorimetria, Instituto de Bioquímica Médica, Universidade Federal do Rio de Janeiro, Rio de Janeiro, RJ, Brazil

[§]Departamento de Bioquímica, Instituto de Biologia, Universidade Estadual de Campinas (UNICAMP), Campinas, SP, Brazil

[∥]Departamento de Biologia e Fisiologia, Faculdade de Medicina de Jundiaí, Jundiaí, SP, Brazil

[⊥]Centro Nacional de Ressonância Magnética Nuclear Jiri Jonas, Instituto de Bioquímica Médica, Universidade Federal do Rio de Janeiro, Rio de Janeiro, RJ, Brazil

[○]Instituto de Física da USP, IFUSP, São Paulo, SP, Brazil

ABSTRACT: Surface tension and isothermal titration calorimetry (ITC) were used to determine the critical micelle concentration (cmc) of the zwitterionic amidosulfobetaine surfactants ASB-14 and ASB-16 (linear-alkylamidopropyldimethylammoniopropanosulfonates) at 25 °C. The cmc and the heat of micellization were determined from 15 to 75 °C by ITC for both surfactants. The increase in temperature caused significant changes in the enthalpy and in the entropy of micellization, with small changes in the standard Gibbs energy (ΔG^{mic}), which is consistent to an enthalpy−entropy compensation with a compensatory temperature of 311 K (ASB-14) and 314 K (ASB-16). In the studied temperature range, the heat capacity of micellization (ΔC_p^{mic}) was essentially constant. The experimental ΔC_p^{mic} was lower than that expected if only hydrophobic interactions were considered, suggesting that polar interactions at the head groups are of significant importance in the thermodynamics of micelle formation by these surfactants. Indeed, a NMR NOESY spectrum showed NOEs that are improbable to occur within the same monomer, resulting from interactions at the polar head groups involving more than one monomer. The ITC and NMR results indicate a tilt in the polar headgroup favoring the polar interactions. We have also observed COSY correlations typical of dipolar interactions that could be recovered with the partial alignment of the molecule in solution, which results in an anisotropic tumbling. The anisotropy suggested an ellipsoidal shape of the micelles, which results in a positive magnetic susceptibility, and ultimately in orientation induced by the magnetic field. Such an ellipsoidal shape was confirmed from results obtained by SAXS experiments that revealed aggregation numbers of 108 and 168 for ASB-14 and ASB-16 micelles, respectively. This study characterizes an interesting micelle system that can be used in the study of membrane proteins by solution NMR spectroscopy.

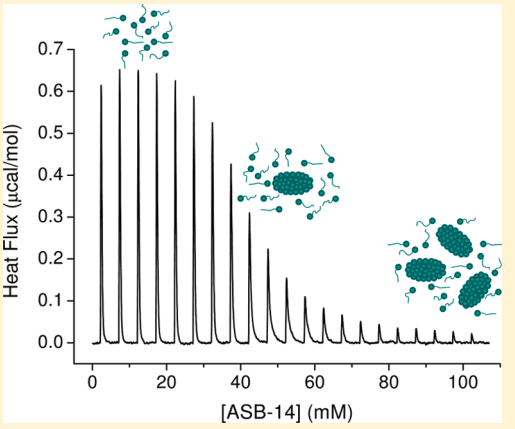

1. INTRODUCTION

Hydrophobic interactions are essential in the self-association of amphiphilic molecules in aqueous solution, but the headgroup also plays an important role on micelle formation. Therefore, the physicochemical properties of a surfactant depend on the hydrophilic−hydrophobic balance of the headgroups and the acyl chains. For ionic micelles, the increase in ionic strength can decrease the electrostatic repulsion between head groups, allowing a low curvature and the formation of larger micelles. Zwitterionic surfactants are electrically neutral, but they bear formally charged groups, presenting a higher polarity than nonionic compounds[1] and properties similar to those of both ionic and noninonic micelles.[1−3] These micelles can bind ions selectively. Zwitterionic sulfobetaine micelles behave as cationic micelles and show a charge gradient between the interior and the interfacial surface. The anion binding increases with decreasing ionic charge density, following the Hofmeister series and the Pearson hard−soft classification.[4−7] Although hexadecylphosphorylcholine (HPC) micelles present an opposite ion-headgroup to that of sulfobetaines, they also incorporate anions in the interfacial region.[5,8] Cuccovia et al.[5] showed that the interfacial anion concentrations in zwitterionic micelles of HPC and 3-(*N*-hexadecyl-*N*,*N*-dimethylammonio) propanesulfonate (HPS) depends on the bulk salt concentration as well as the dipole orientation of the detergent headgroup and the nature of the cations.

Received: September 19, 2010
Revised: December 27, 2010
Published: June 09, 2011

Scheme 1. Chemical Structure of the Zwitterionic Amidosulfobetaine Surfactants

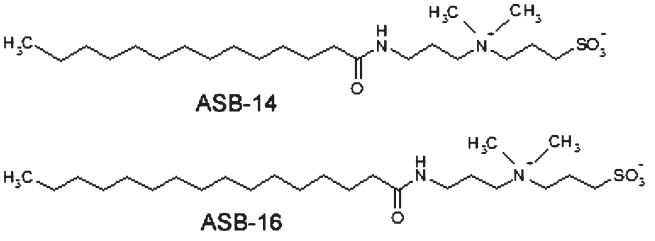

The critical micelle concentration (cmc) and the aggregation number (N) are important properties of surfactants that depend on experimental conditions. The cmc of a surfactant can be determined by surface tension,[9−12] dye solubility,[10−13] light scattering,[14−16] electrical conductivity,[15−17] and spin label mobility.[18] By using isothermal titration calorimetry (ITC) it is possible to measure both the cmc and the enthalpy of micellization,[19−33] allowing a more accurate calculation of the entropy and the free energy involved in the process.

The zwitterionic detergents with an amidosulfobetaine headgroup and alkyl tails of 14 (ASB-14) and 16 (ASB-16) carbon atoms have been described as very effective for the solubilization of membrane proteins.[34−37] Despite their recognized biological application, only a preliminary study of the micellization of these surfactants was done at 25 °C by electron spin resonance.[18]

In this work we describe the physicochemical characterization of the ASBs micelles by different techniques. The thermodynamics of micelle formation for both ASB-14 and ASB-16 was studied by high sensitivity titration calorimetry (ITC) in a wide temperature range (from 15 to 75 °C). Molecular details on the micelle organization were revealed by NMR measurements, whereas the micellar shape, size and aggregation number N were determined by small-angle X-ray scattering.

2. MATERIALS AND METHODS

2.1. Materials. The zwitterionic amidosulfobetaine detergents tetradecanoylamido propyl dimethyl ammonio propanesulfonate (ASB-14) and hexadecanoylamido propyl dimethyl ammonio propanesulfonate (ASB-16) were obtained from Calbiochem, La Jolla, CA, and used without further purification. The structures of these surfactants are shown in Scheme 1. All other reagents were of analytical grade.

2.2. Surface Tension. Surface tension was measured in a Sigma-701 tensiometer from KSV Instruments Ltd. (Helsinki, Finland). ASB-14 and ASB-16 solutions with concentrations ranging from 1 to 500 μM were used. Briefly, the surface tension (γ) of the liquid is measured prior to any addition of the surfactant and after each addition and solubilization of a determined amount of surfactant. The cmc was calculated from the semilogarithmic plot of surface tension as a function of the surfactant bulk concentration.

2.3. Isothermal Titration Calorimetry. Heats of dilution and demicellization of ASB-14 and ASB-16 were measured in a VP-ITC from MicroCal, Llc (Northamptom, MA, USA) from 15 to 75 °C. At 10 °C the signal obtained with both surfactants was poor with fluctuations in the heat effect, and the data were not analyzed. The principles of the technique were described by Wiseman et al.[38] Aliquots of micellar solution of each surfactant were injected at 5 min intervals into the sample cell (V = 1.422 mL) filled with Milli-Q water, under continuous stirring at 300 rpm. The thermograms of the heats of dilution of the detergents were analyzed with the ORIGIN 5.0 software provided by MicroCal. The cmc was determined by the minimum of the first derivative of the curve obtained for the enthalpy of detergent dilution as a function of total detergent concentration in the cell. The initial concentration of ASB-14 in the syringe was 5 mM. For ASB-16, the concentration in the syringe was 0.21 mM for the titrations up to 45 °C, and 1 mM from 55 to 75 °C.

2.4. Nuclear Magnetic Resonance. The NMR spectra were acquired in a Bruker DRX 400 MHz and/or a Bruker Avance III 800 MHz at 25 °C. NMR samples of ASB-16 (45 mM) and ASB-14 (45 mM and 500 mM) were prepared in Milli-Q water containing 10% ^2H_2O. Phase sensitive NOESY[39] and TOCSY[40] spectra were acquired at 9.4 T (400.13 MHz) with presaturation for solvent suppression, 4,096 complex points in F2, and 512 complex points in F1; quadrature detection in the indirect dimension was obtained by States-TPPI method.[41] A mixing time of 50 and 100 ms was used for the NOESY spectra and 69.7 ms of spin lock[40] for the TOCSY experiments. Both spectra were processed using Topspin 2.1. COSY[42] spectra were acquired at 9.4 T (400.13 MHz) in magnitude mode with 4,096 complex points in F2 and 256 points in F1. The spectra were processed using squared sine bell as window function with zero filling doubling the number of points. $^{13}C-^{1}H$ splitting due to scalar and residual dipolar coupling were measured using coupled HSQC spectra at two fields (18.8 and 9.4 T). We used gradient selected HSQC[43] with 2,048 complex points in F2 and 512 complex points in F1. Echo/antiecho TPPI[44] mode was used for quadrature detection in the indirect dimension; the sweep width was 15 ppm for ^1H centered in water and 70 ppm for ^{13}C centered at 40 ppm. To obtain the coupled HSQCs, the 180° ^1H pulse in the middle of ^{13}C evolution was abolished. Fully decoupled HSQCs were also acquired as a control.

2.5. Small-Angle X-ray Scattering. SAXS experiments were performed at the National Laboratory of Synchrotron Light (LNLS, Campinas, SP, Brazil) at room temperature (22 ± 1 °C), with radiation wavelength λ = 1.488 Å and sample-to-detector distance of ∼900 mm. Micelle aqueous solutions of 50 mM ASB-14 and ASB-16, were prepared in Milli-Q water. Samples were set between two mica windows, 1 mm spacer, handled in a liquid sample-holder, and placed perpendicular to the X-ray beam. The obtained images (two-dimension position sensitive detector) were radially averaged and normalized by taking into account the decrease in the intensity of the X-ray beam during the experiment and the time for the measurements (data acquisition of 15 min).

The SAXS intensity $I(q)$ of an isotropic solution of noninteracting spheroidal particles of low anisometry (smaller than 3) can be described as[47−49]

$$I(q) = kn_pP(q) \quad (1)$$

where n_p and k correspond to the particle number density and the normalization factor related to the instrumental effects, respectively. The scattering vector $q = (4\pi/\lambda)\sin\theta$, in which 2θ is the scattering angle and λ is the wavelength of the X-rays. $P(q)$ corresponds to the orientational average of the scattering particle form factor. In the case of the ASBs, the micelle form factor $P(q)$ is represented by a prolate ellipsoid of two shells of different electron densities ρ in respect to the solvent electron density.[48,49] In this work, ρ_w = 0.333 e/Å^3 for water. The prolate micelle, with axial ratio ν, is represented by a hydrophobic paraffinic core with electron density ρ_{par} = 0.275 e/Å^3, being the shortest semiaxis on the order of the paraffinic chain length, R_{par}, and the longest semiaxis defined as νR_{par}. The hydrophobic core is surrounded by a polar shell of thickness σ and electron density ρ_{pol}, which includes the polar head groups and hydration water. The structural parameters R_{par}, ν, σ, and ρ_{pol} are obtained by the fitting of the experimental data to eq 1. We used the Global fitting procedure (GENFIT software)[50−54] that performs a χ^2 minimization with a simulating annealing process,[56] changing the free parameters until χ^2 reaches a minimum value. This allows the linkage among different fitting parameters from distinct scattering curves. This process improves the uniqueness of the final solution. Once R_{par} and ν are determined, the micellar aggregation number, N, can be calculated by

dx.doi.org/10.1021/la1037525 |Langmuir 2011, 27, 8248–8256

Table 1. Effect of the Temperature on the Critical Micelle Concentration (cmc) and Thermodynamic Parameters of Micellization of ASB-14 and ASB-16

compound	T (°C)	cmc (mM)	ΔH^{mic} (kJ·mol^{-1})	ΔG^{mic} (kJ·mol^{-1})	$T\Delta S^{mic}$ (kJ·mol^{-1})
ASB-14	15	0.128 ± 0.010	1.24 ± 0.05	−31.09 ± 0.18	32.36 ± 0.15
	20	0.109 ± 0.006	−1.50 ± 0.05	−31.46 ± 0.12	29.96 ± 0.12
	25	0.119 ± 0.004	−3.85 ± 0.05	−32.34 ± 0.08	29.25 ± 1.78
	25[a]	0.115[a]			
	30	0.104 ± 0.046	−6.28 ± 0.05	−32.25 ± 0.07	25.95 ± 0.09
	35	0.147 ± 0.009	−8.37 ± 0.17	−32.93 ± 0.15	24.58 ± 0.14
	40	0.148 ± 0.003	−10.39 ± 0.22	−32.87 ± 0.05	22.23 ± 0.39
	45	0.169 ± 0.006	−12.79 ± 0.45	−33.58 ± 0.10	20.74 ± 0.58
	55	0.204 ± 0.016	−16.93 ± 1.97	−34.14 ± 0.21	17.08 ± 1.90
	65	0.262 ± 0.022	−21.16 ± 1.41	−34.48 ± 0.24	13.25 ± 1.18
	75	0.349 ± 0.032	−25.02 ± 2.81	−34.67 ± 0.27	9.64 ± 2.54
ASB-16	15	0.0104 ± 0.0093	1.39 ± 0.33	−37.37 ± 0.05	38.76 ± 1.1
	20	0.00854 ± 0.0007	−3.89 ± 0.18	−37.58 ± 0.20	33.93 ± 0.21
	25	0.0096 ± 0.0003	−5.56 ± 0.34	−38.59 ± 0.09	33.03 ± 0.38
	25[a]	0.011[a]			
	30	0.0101 ± 0.002	−7.00 ± 0.69	−38.78 ± 0.22	31.40 ± 0.73
	35	0.0115 ± 0.0011	−9.92 ± 0.68	−39.29 ± 0.34	29.56 ± 0.99
	40	0.116 ± 0.0021	−11.39 ± 1.36	−39.41 ± 0.36	27.86 ± 1.63
	45	0.0147 ± 0.0013	−15.11 ± 1.30	−40.07 ± 0.32	25.07 ± 0.91
	55	0.0213 ± 0.0029	−21.71 ± 0.61	−40.31 ± 0.36	18.87 ± 1.12
	65	0.0272 ± 0.0023	−25.22 ± 0.64	−40.84 ± 0.24	15.62 ± 1.38
	75	0.037 ± 0.0016	−29.9 ± 0.32	−41.12 ± 0.12	13.27 ± 1.21

[a] Values determined by surface tension.

taking into account the volume of the ellipsoidal micelle hydrophobic core

$$4\pi\nu(R_{par})^3/3 = NV_{par} \quad (2)$$

with $V_{par} = 27.4 + 26.9n_C$, the hydrophobic volume of linear surfactant with n_C carbon atoms in the alkyl chain.[57] The hydration number per polar head, W, can be further evaluated from the combined values of N, σ, and ρ_{pol}. Details can be found elsewhere.[49,56]

3. RESULTS AND DISCUSSION

3.1. Critical Micelle Concentration. Table 1 shows the cmc values for ASB-14 and ASB-16 determined by surface tension measurements at 25 °C (Figure 1) and by ITC from 15 to 75 °C. The cmc values obtained by surface tension were very similar to those previously determined by ESR[18] and to the ones determined by ITC (Table 1).

Figure 2 illustrates a typical ITC experiment of the demicellization of ASB-14, where a solution of ASB-14 micelles was injected into the calorimetric cell containing water. In the first seven injections, the endothermic peaks from these injections were due to: (*i*) the heat of dilution of micelles and monomers in solution and (*ii*) the heat due to the disruption of the micelles. As the surfactant concentration increased, the heat effect due to the demicellization gradually decreased and the final injections reflect the heat of dilution of micelles and monomers. The heat flux as a function of time was integrated from the baseline and the area under each peak was normalized for the number of moles of injectant in the cell. These integrations gave rise to the sigmoid curve in Figure 2B of the calorimetric enthalpy (ΔH_{cal}) as a function of the surfactant concentration. The enthalpy of demicellization (ΔH_{demic}) was calculated as the difference between the average enthalpy obtained above the cmc and that obtained below the cmc. ΔH_{demic} is equal in number but opposite in sign to the enthalpy of micelle formation (ΔH_{mic}). Cmc values were determined from the minimum in the first derivative of the sigmoid curve of ΔH_{cal} as a function of ASB concentration (Figure 2C).

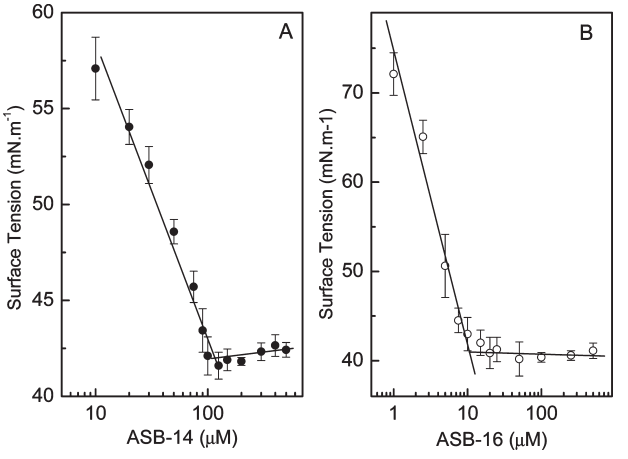

Figure 1. Surface tension as a function of bulk concentration of ASB-14 (A) and ASB-16 (B) at 25 °C in Milli-Q water. The cmc corresponds to the surfactant concentration where maximally reduced surface tension is achieved.

The effect of the temperature on the cmc of both ASB-14 and ASB-16 is shown in Figure 3 and the data is summarized in Table 1. As expected, cmc values of ASB-16 were lower than those for ASB-14 (Table 1 and Figure 3).

The cmcs of both ASB-14 and ASB-16 are lower than that determined in water at 25 °C for the sulfobetaines SB-14 (0.25 mM[57] and

dx.doi.org/10.1021/la1037525 |*Langmuir* 2011, 27, 8248–8256

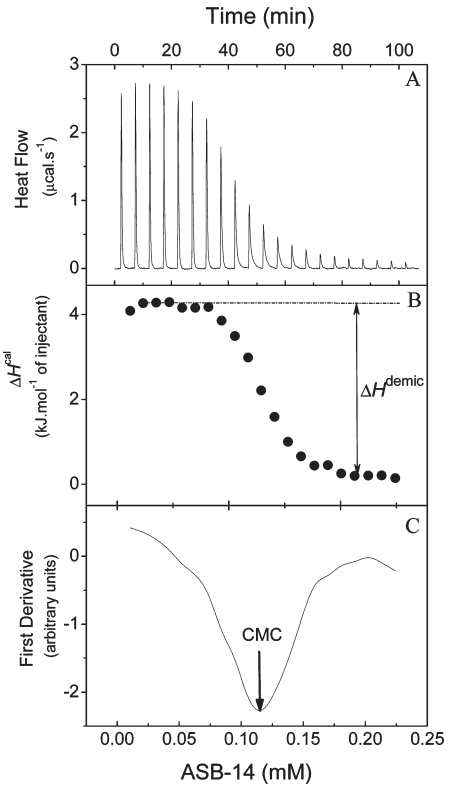

Figure 2. Titration of ASB-14 micellar solution (5 mM) into the calorimetric cell (1.422 mL) containing water at 25 °C. (A) Heat flow as a function of time for 24 injections of 3 μL ASB-14 into Milli-Q water. (B) Reaction enthalpy (ΔH^{cal}) as a function of ASB-14 final concentration in the cell where the ΔH^{demic} is indicated by an arrow. (C) First derivative of curve B where the minimum corresponds to the cmc.

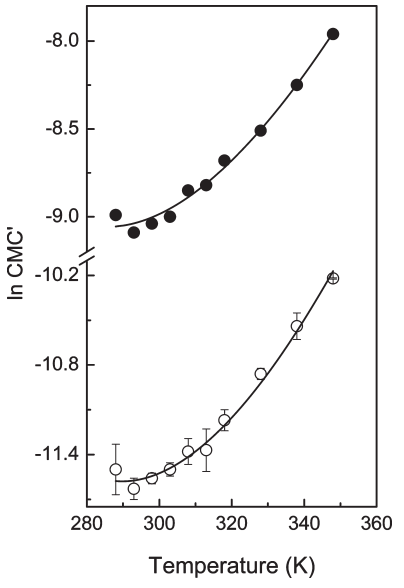

Figure 3. Effect of temperature on cmc′ for ASB-14 (●) and ASB-16 (○). The solid lines represent the curve fitting according to eq 3.

0.27 mM[58]) and SB-16 (0.028 mM[57,58]), suggesting that the amide group favors the micellization.

3.2. Thermodynamics of Micelle Formation. The effect of temperature on the thermodynamic parameters of micellization

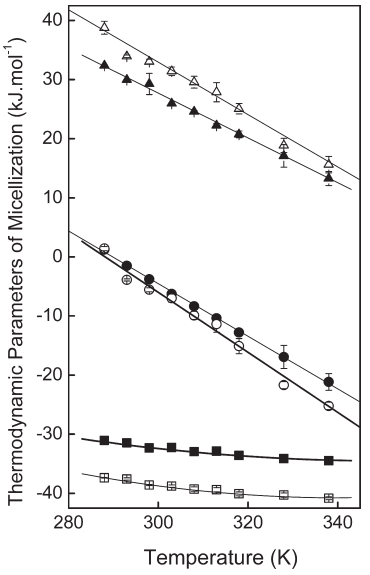

Figure 4. Thermodynamic parameters for micelle formation of ASB-14 (solid symbols) and ASB-16 (open symbols) in Milli-Q water as a function of the temperature. Solid lines represent the best fits of the experimental data. ΔH^{mic} (●, ○) was fitted according to eq 9; $T\Delta S^{mic}$ (▲, Δ) was fitted by a linear correlation and ΔG^{mic} (■, □) by a second degree polynomial.

of ASB-14 and ASB-16 is shown in Figure 4, and it is summarized in Table 1. For both surfactants, the micellization was endothermic at 15 °C and exothermic from 25 to 75 °C.

Assuming a pseudophase separation model, the standard Gibbs energy of transfer of a monomer from water to a micelle (ΔG^0_{mic}, Figure 4 and Table 2) can be calculated from the van't Hoff equation:

$$\Delta G^0_{mic} = -RT \ln \mathrm{cmc}' \quad (3)$$

where cmc′ is the critical micelle concentration in mole fraction units. Equation 3 leads to the correlation between the cmc and the enthalpy of micelle formation:

$$\Delta H^{mic} = -RT^2 \frac{\partial(\ln \mathrm{cmc}')}{\partial T} \quad (4)$$

The van't Hoff enthalpy at 25 °C (ΔH^0) and the heat capacity change (ΔC^0_p) of micellization were calculated from the temperature dependence of the cmc′ (Table 2):

$$\ln(\mathrm{cmc}') = a + \frac{b}{T} + c \times \ln T \quad (5)$$

$$\Delta H^\circ = R(-b + cT) \quad (6)$$

$$\Delta C^0_p = Rc \quad (7)$$

For both surfactants, ΔH^0 obtained from eq 6 was close to the ΔH_{mic} obtained by ITC at 25 °C (Table 1). ΔH^0 and ΔC^0_p (Table 2) where also calculated according to Kresheck[26] from the molar enthalpy change (ΔH_{R}) and the heat capacity change ($\Delta C_{p_{\mathrm{R}}}$) at a reference temperature (T_{R} = 298 K), by fitting the experimental data to:

$$\Delta H^\circ = \Delta H_R + (\Delta C_{p_R} - BT_R)(T - T_R) + \frac{B}{2}(T^2 - T_R{}^2) \quad (8)$$

dx.doi.org/10.1021/la1037525 |*Langmuir* 2011, 27, 8248–8256

Table 2. Thermodynamic Parameters of Micelle Formation for ASB-14 and ASB-16

compound	n_{CH_2}*(mon)[a]	ΔC_p^{mic},[a] J/mol·K	B coefficient, J/mol·K[b]	ΔH^0,[c] kJ/mol	$\Delta C_p{}^0$,[c] J/mol·K^{-1}
ASB-14	13.5	-480 ± 7	-1.385 ± 0.6	4.64 ± 1.2	-524 ± 10
ASB-16	15.5	-605 ± 45	-1.596 ± 0.8	7.69 ± 1.7	-713 ± 59

[a] n_{CH_2}*(mon) is the effective number of methylenes driving self-association, and it was calculated as described in the text, considering 1 for each methylene group, and 1.5 for methyl groups. [b] ΔC_p^{mic} is the heat capacity change for micelle formation calculated from the fitting to eq 9 of the temperature dependence of ΔH^{mic} (Figure 4). [c] ΔH^0 and $\Delta C_p{}^0$ values were calculated from the fitting of the curves obtained for ln CMC' as a function of temperature according to eq 6 and 7, respectively.

where

$$\Delta C_p^0 = \Delta C_{p_R} + B(T - T_R) \quad (9)$$

The entropic term for micellization ($T\Delta S_{mic}$, Figure 4 and Table 2) was, then, calculated by the Gibbs−Helmholtz equation:

$$\Delta G_{mic}^0 = \Delta H_{mic} - T\Delta S_{mic} \quad (10)$$

The enthalpy−entropy compensation in the micellization of both ASB-14 and ASB-16 can be better visualized in Figure 4. Similar to that found for other compounds,[27−32] the micelle formation of ASB-14 and ASB-16 was enthalpy-driven at higher temperatures and characterized by a large and negative ΔG_{mic}^0 that did not significantly change with temperature (Figure 4 and Table 1).

Entropy-enthalpy compensation was first described by Lumry and Rajender[59] in which a proportionality constant, defined as the compensation temperature, was found in a narrow range, from about 250 to 315 K, for different processes. The entropy-enthalpy compensation in micelle formation can be explained by the interplay between the water molecules in contact with the acyl chains (solvation or "bound" water) and the bulk water molecules ("free" water). With the increase in temperature, the exchange between "bound" and "free" water is easier than it is at lower temperatures. As a consequence, the entropic contribution decreases with the temperature and the slope from the curve of ΔS_{mic} as a function of ΔH_{mic} gives the compensation temperature. Sugihara and Hisatomi[60] calculated the compensation temperature for more than 15 nonionic, anionic, and cationic surfactants and found a compensation temperature ranging from 299 to 315 K, depending on the species. In this work, we found very similar values with a compensation temperature of 311 K for ASB-14 and 314 for ASB-16.

An approximate value for $\Delta\Delta G_{mic}$ and $\Delta\Delta H_{mic}$ per methylene group was calculated from the plots of ΔG_{mic} and ΔH_{mic} obtained at 25 °C as a function of the effective methylene number, nCH$_2$*(mon). According to Heerklotz and Epand,[30] this number considers only methylene groups that are exposed to water in the monomeric form, the methyl group counting as 1.5. Thus, nCH$_2$*(mon) is 13.5 for ASB-14 and 15.5 for ASB-16. The incremental $\Delta\Delta G_{mic}$ per methylene group ($\Delta\Delta G_{mic} = -3.13$ kJ·mol^{-1}) found for the ASBs is in a very good agreement to those reported for other surfactants.[30] The incremental enthalpy per methylene group at 25 °C was -0.86 kJ·mol^{-1}. From the relation $\Delta\Delta G = \Delta\Delta H - T\cdot\Delta\Delta S$, the entropic term found here ($-T\Delta\Delta S = -2.27$ kJ·mol^{-1}) was similar to the -3 kJ·mol^{-1} reported for liquid hydrocarbons.[30]

For ionic surfactants the interactions at the polar headgroup region should also be considered. Therefore, the enthalpy and the Gibbs free energy of micellization are not only a result of contributions from the acyl chains. Depending on the conformation of the head groups upon formation of the electrical double layer one can expect to have Coulombic repulsions due to the surfactant headgroup charges. Nevertheless, favorable interactions can also take place. In order to evaluate the energetic of the headgroup contribution of the ASBs upon micelle formation, we analyzed changes in heat capacity.

3.3. Heat capacity changes and methylene group contributions. The heat capacity changes on micelle formation (ΔC_p^{mic}, Table 2) is a temperature dependent variable,

$$\langle \Delta C_p \rangle = \delta \langle \Delta H_{mic} \rangle / \delta T \quad (11)$$

and in the temperature range studied here, we found a good linear correlation of ΔH_{mic} as a function of temperature. However, a better fitting was achieve with the nonlinear model (eq 9) described by Kresheck[26] (Figure 4 and Table 2).

ΔC_p^{mic} for the ASBs were smaller than the expected from the empirical correlation determined from the dissolution of hydrocarbons.[61] This behavior was also observed for other surfactants.[22,24,30] Considering this empirical correlation, in which $\Delta C_p = 33\ n_H$ (J·mol^{-1}·K^{-1}), where n_H is the number of hydrogen atoms exposed to water, one could expect a $\Delta C_p^{mic} = -891$ J·mol^{-1}·K^{-1} for ASB-14 and $\Delta C_p^{mic} = -1023$ J·mol^{-1}·K^{-1} for ASB-16. Heat capacity were obtained in two ways: ΔC_p^0 from the temperature dependence of the cmc′ (eq 6, Table 2) and ΔC_p^{mic} from the temperature dependence of ΔH^{mic}. ΔC_p^0 values are higher than ΔC_p^{mic} obtained from ITC data (Table 2). Nevertheless, both values obtained from the experimental data are significantly lower than the predicted ones from the empirical correlation from dissolution of hydrocarbons shown above.

The discrepancy in the methylene contributions to the thermodynamic parameters of micellization could be an indication that at least half of the methylene groups are exposed to water after micelle formation. This would lead to very unstable aggregates if one considers the contribution of the amidosulfobetaine headgroup. We suggest that the micelles are also stabilized by intermolecular interactions at the headgroup region between neighboring surfactants, i.e., by the formation of a salt bridge between the quaternary amine group of one surfactant and the sulfonate group of another surfactant, as well as the formation of a hydrogen bond between the amide groups of these surfactants. This is possible if the head groups are not tethered as it occurs with sulfobetaines, where the highly hydrophilic sulfonate group is located at the micelle surface while the less hydrophilic quaternary amine is located near the hydrocarbon region of the micelle.[62] The conformation of the ASBs micelles are more similar to that observed with hexadecyl phosphorylcoline (HPC)[8] micelles and in bilayers of phosphatidylcholine (PC) or phosphatidylethanolamine (PE).[63,64]

3.4. NMR Studies of the ASB Micelles. In order to better understand the interactions at the polar headgroup region in both ASBs micelles, we used NMR spectroscopy. We have fully assigned ^{1}H and ^{13}C nuclei of ASB-14 and ASB-16. A NOESY spectrum of 100 ms mixing time showed several NOEs connecting adjacent hydrogens (Figure 5, solid arrows) within the

dx.doi.org/10.1021/la1037525 |Langmuir 2011, 27, 8248–8256

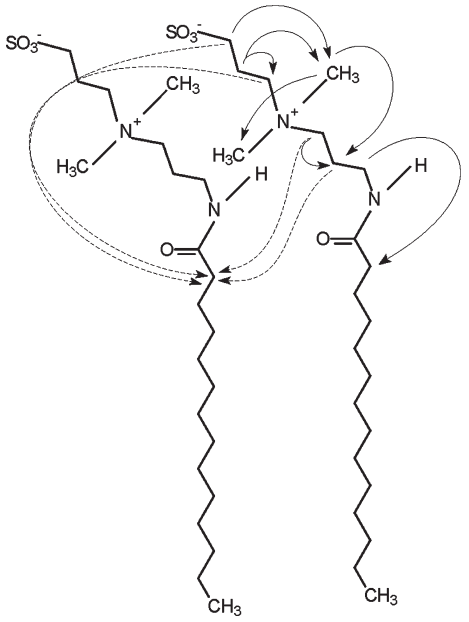

Figure 5. Representation of the nuclear Overhauser cross-peaks detected between hydrogens of the polar headgroup region of ASB detergents.

surfactant monomer. We also observed NOEs that are improbable to occur within the same monomer. We interpreted these NOEs as a result of interactions involving more than one monomer, as depicted in Figure 5 by dotted arrows. Therefore, the micelles formed by both ASB-14 and ASB-16 displayed intermolecular NOEs that evidence polar head tilts, which are represented in Figure 6. This finding is in agreement with the prediction from the discrepancies of the experimental and predicted ΔC_p that suggested polar interactions between adjacent monomers.

We assigned both surfactants using COSY correlations (Figure 6). We have noticed the expected COSY correlation through scalar coupling involving adjacent hydrogens linked by three bonds. Remarkably, we have also observed the presence of COSY correlations involving hydrogens that are not linked to adjacent carbons. These correlations are typical of dipolar interactions, rather than the interaction that results from scalar coupling. In solution, dipolar coupling is zero for isotropic solutions since it is averaged due to isotropic molecular tumbling. In the case of the ASBs, dipolar coupling is higher than zero, meaning that it is not completely averaged. This suggests a partial alignment of the micelle in solution resulting in anisotropic tumbling. The anisotropy could be explained by an ellipsoid shape of the micelles, which results in a positive magnetic susceptibility vector, and ultimately in orientation induced by the magnetic field.

To confirm the orientation by an independent parameter, we measured the $^{13}C-^{1}H$ splitting for each hydrogen in the molecule (Table 3). If the splitting was only due to $^{1}J_{CH}$, it would be independent of the magnetic field. However, we observed that the splitting changed with the magnetic field due to different degrees of orientation in the different fields. We actually measured the sum of the scalar coupling and residual dipolar coupling ($^{1}J_{CH} + {}^{1}D_{CH}$). Residual dipolar coupling ($^{1}D_{CH}$), that is a consequence of the partial alignment, is the parameter that varies with the magnetic field, since the residual alignment tends to increase with the magnetic field.

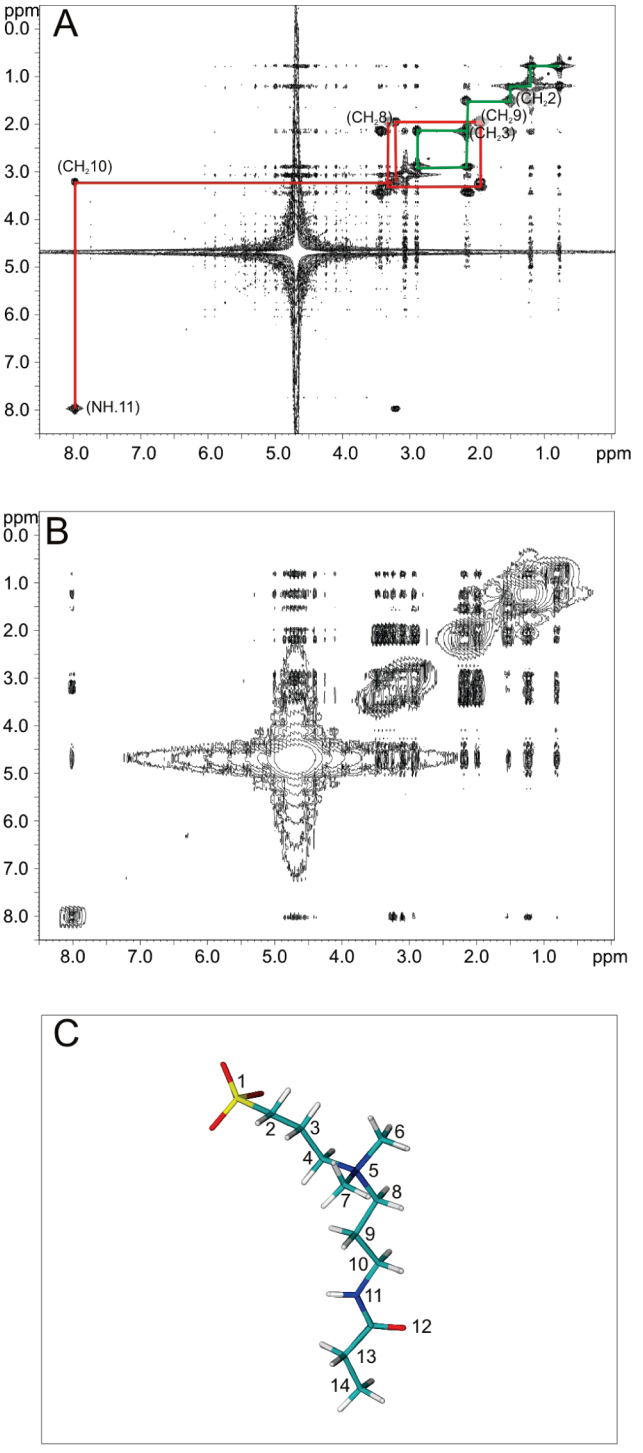

Figure 6. NMR correlation spectroscopy (COSY) spectra of the ASB-14. (A) COSY spectrum of 45 mM ASB-14. The red lines show the through bond conectivities used for the assignment of the surfactant. (B) COSY spectrum of 500 mM ASB-14. The increase in concentration evidence the correlations via residual dipolar coupling. (C) Model of ASB-14 headgroup with the number of each heavy atom to serve as a reference for the visualization of the COSY spectra and Table 3 that contains the full assignment. The spectra were obtained at 25 °C.

We have also tested if the orientation was due to crowding effects, rather than magnetically induced. The observed $^{13}C-^{1}H$ splitting was the same for ASB-14 at 50 mM and 500 mM (data not shown),

dx.doi.org/10.1021/la1037525 |*Langmuir* 2011, 27, 8248–8256

Table 3. Scalar Couplings ($^1J_{CH}$) of ASB-14 (A) and ASB16 (B) Measured at 19.2 and 9.6 T[a]

A	chemical group	$^1J_{CH}$, Hz 800 MHz	$^1J_{CH}$, Hz 400 MHz	ΔJ (Hz)	ppm
1	SO_3	-	-	-	-
2	CH_2	268.87	273.84	- 4.97	2.89
3	CH_2	255.20	257.78	- 2.58	2.15
4	CH_2	302.54	289.20	- 13.34	3.43
5	CH_3	253.99	252.16	3.63	1.18
6	CH_3				0.77
7	N	-	-	-	-
8	CH_2	293.11	289.03	4.08	3.30
9	CH_2	261.61	258.18	3.43	1.92
10	CH_2	276.11	280.88	- 4.77	3.21
11	NH	-	-	-	7.97
12	CO	-	-	-	-
13	CH_3				3.05

B	chemical group	800 MHz	400 MHz	$\Delta\upsilon$ (Hz)	ppm
1	SO_3	-	-	-	
2	CH_2	268.87	273.84	- 4.97	
3	CH_2	255.20	257.78	- 2.58	
4	CH_2	302.54	289.20	- 13.34	
5	CH_3	253.99	252.16	3.63	
6	CH_3				
7	N	-	-	-	
8	CH_2	293.11	289.03	4.08	
9	CH_2	261.61	258.18	3.43	
10	CH_2	276.11	280.88	- 4.77	
11	NH	-	-	-	
12	CO	-	-	-	
13	CH_3				

[a] The difference ΔJ (Hz) reflects the partial orientation of both micelles induced by the magnetic field. The assignment of each hydrogen in the ASBs molecules is in the fifth column.

implicating that the orientation is exclusively due to the magnetic susceptibility of the micelle. The results thus suggested that the micelles of ASB-14 and ASB-16 are not spherical, which can be an advantage to the application of these micelles to study structural properties of proteins by NMR. In order to better explore the structural features of ASB-14 and ASB-16 micelles, SAXS measurements were then performed, as follows.

3.5. SAXS studies of the ASB micelles. Figure 7 shows the SAXS curves of ASB-14 and ASB-16 along with the best fittings to the experimental data (eq 1), and the fitting parameters are described in Table 4. The experimental data are well represented by the scattering profile of prolate ellipsoid micelles for both surfactants. It corroborates the NMR results that indicated an ellipsoid shape for both micelles.

The micelle structural parameters are similar for both surfactants concerning the polar shell features and the ellipsoid axial ratio (Table 4). The main difference resides on the paraffinic radius, R_{par}, which is shorter for ASB-14, as expected. The R_{par} values are in very good agreement with those obtained for C14 and C16 extended chain length of 19.2 and 21.7 Å, respectively ($l_c = 1.5 + 1.265n_c$). Therefore, the interface between the polar and apolar regions of the micelle must reside near the carboxyl

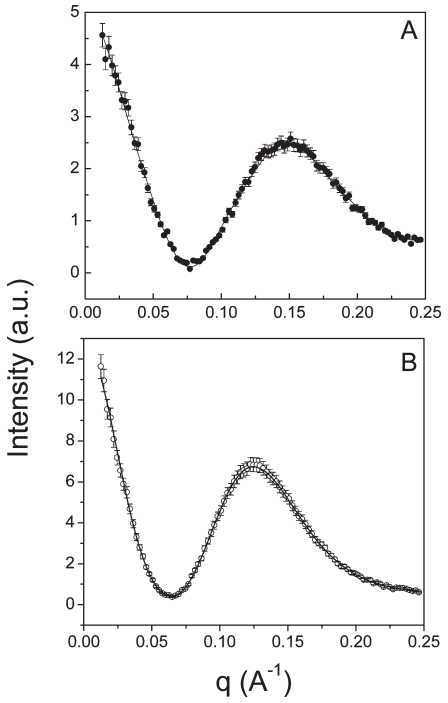

Figure 7. SAXS curves of 50 mM ASB-14 (A) and 50 mM ASB-16 (B). The solid lines represent the best fittings obtained with the ellipsoidal model. See text for details. The fitting parameters are described in Table 4.

Table 4. Fitting Parameters Obtained from the Scattering Curves of Samples Composed of 50 mM of ASB-14 and ASB-16 in Water Using the Ellipsoidal Model[a]

surfactant	R_{par} (Å)	σ (Å)	ρ_{pol} (e/Å^3)	ν	N	W
ASB14	18.0(5)	8.1(5)	0.391(7)	1.80(2)	108(12)	12
ASB16	21.7(5)	9.1(6)	0.392(7)	1.80(2)	168(13)	13
LPC[b]	22.5(3)	9.0(2)	0.39(1)	1.6(1)	166(13)	11
HPS[b]	22.5(3)	7.4(4)	0.39(1)	1.6(1)	166(13)	11

[a] R_{par} is the paraffinic radius, σ and ρ_{pol} are the thickness and the electronic density of the polar headgroup, respectively, ν is the ratio between the largest and the shortest semiaxes of the ellipsoid, N and W are the micellar aggregation number and the number of water molecules per surfactant molecule into the polar shell, respectively.* Values extracted from the literature.[51,66] The uncertainties are represented in parentheses.

group (C═O region, see Scheme 1). Considering the extended chain length of the polar head of about 13.2 Å and the observed thickness of the polar head of 8.1 Å for ASB-14 and 9.1 Å for ASB-16, we estimated the polar head tilt angle as 38° for ASB-14 and 44° for ASB-16. The shortest hydrophobic semiaxis dimensions are compatible to the respective extended alkyl chain lengths.

The aggregation numbers (N) found for ASB-14 and ASB-16 were 108 and 168, respectively (eq 2, Table 4), which are considerably higher than that observed for sulfobetaines where N was reported as 60 by Di Profio et al.[3] for SB-14, and 67 for SB-14 and 71 for SB-16 by Graciani et al.[58]

Considering the ASBs N values and the polar shell thickness σ, *circa* 12 water molecules must be hydrating each amidosulfobetaine polar head (Table 4). For comparison, Table 4 also contains the structural parameters determined for two other zwitterionic

dx.doi.org/10.1021/la1037525 |*Langmuir* 2011, 27, 8248–8256

surfactants, 3-(*N*-hexadecyl-*N*,*N*-dimethyl-3-ammonium) propanesulfonate (HPS) and L-α-lysophosphatidylcholine (LPC), both having the same hydrophobic contribution of ASB-16. Note however that, in spite of the differences in the polar head groups, LPC, HPS, and ASB-16 present similar values of R_{par} and ν. As a consequence, the aggregation numbers are also quite similar (Table 4). This fact suggests that, although the micellization of the ASBs is driven by hydrophobic contribution and polar head interaction, the aggregation number depends mainly on the length of the hydrophobic paraffinic tail.

4. CONCLUSIONS

The thermodynamics of micelle formation of the amide sulfobetaine surfactants ASB-14 and ASB-16 showed enthalpy−entropy compensation as already observed with other surfactants. The thermodynamic data indicated that headgroup interactions play an important role to the micelle formation and stability. It is important to note that the discrepancies in the heat capacity values obtained from the experimental data and from the theoretical estimation suggested the orientation of the polar headgroup. This conformation as showed by direct NOE observation (NMR) and by the structural SAXS parameters, as seen by the tilt angle of about 40° at the polar head groups of the ASBs. NMR dipolar coupling measurements provided information on the anisotropic character of the ASBs micelle, which was corroborated by the SAXS determination of the ellipsoid structure of ASBs micelles.

This work shows that ASB-14 and ASB-16 are good candidates for membrane protein solubilization. In addition, the observed anisotropy can be useful for the measurement of residual dipolar couplings in solution NMR structural determination.

AUTHOR INFORMATION

Corresponding Author

*Address: Laboratório de Biocalorimetria, IBQM/UFRJ, Prédio do CCS - Bloco e - Sala 27b, Rio de Janeiro, RJ 21941-290, Brazil. Telephone: +55 21 3717-5176. Fax: +55 21 2270-8647. E-mail: bianconi@bioqmed.ufrj.br or lucia.bianconi@gmail.com.

Author Contributions

‡Both authors contributed equally to this work and should be considered as first authors.

ACKNOWLEDGMENT

This work was supported by research grants from Financiadora de Estudos e Projetos (FINEP/CT-Infra), Conselho Nacional de Desenvolvimento Científico e Tecnológico (CNPq), Fundação Carlos Chagas Filho de Amparo à Pesquisa do Estado do Rio de Janeiro FAPERJ, and Fundação de Amparo à Pesquisa do Estado de São Paulo (FAPESP). M.G.D and C.C.D. acknowledge the fellowships from CNPq and Coordenação de Aperfeiçoamento de Pessoal de Ensino Superior (CAPES). We thank Dr. Watson Loh for facilities.

REFERENCES

(1) Laughlin, R. G. *Langmuir* **1991**, *7*, 842.
(2) Correia, V. P.; Cuccovia, I. M.; Stelmo, M.; Chaimovich, H. *J. Am. Chem. Soc.* **1992**, *114*, 2144.
(3) Di Profio, P.; Germani, R.; Savelli, G.; Cerichelli, G.; Chiarini, M.; Mancini, G.; Bunton, C. A.; Gillitt, N. D. *Langmuir* **1998**, *14*, 2662.
(4) Baptista, M. S.; Cuccovia, I.; Chaimovich, H.; Politi, M. J.; Reed, W. F. *J. Phys. Chem.* **1992**, *96*, 6442.
(5) Cuccovia, I. M.; Romsted, L. S.; Chaimovich, H. *J. Colloid Interface Sci.* **1999**, *220*, 96.
(6) Tondo, W. T.; Priebe, J. M.; Souza, B. S.; Priebe, J. P.; Bunton, C. A.; Nome, F. *J. Phys. Chem. B* **2007**, *111*, 11867.
(7) Farrukh, M. A.; Beber, R. C.; Priebe, J. P.; Satnami, M. L.; Micke, G. A.; Costa, A. C. O.; Fiedler, H. D.; Bunton, C. A.; Nome, F. *Langmuir* **2008**, *24*, 12995.
(8) Priebe, J. P.; Souza, B. S.; Micke, G. A.; Costa, A. C. O.; Fiedler, H. D.; Bunton, C. A.; Nome, F. *Langmuir* **2010**, *26*, 1008.
(9) Blandamer, M. J.; Briggs, B.; Cullis, P. M.; Engberts, J. B. F. N.; Kevelam, J. *Phys. Chem. Chem. Phys.* **2000**, *2*, 4369.
(10) Blandamer, M. J.; Cullis, P. M.; Soldi, L. G.; Engberts, J. B. F. N.; Kacperska, A.; van Os, N. M.; Subha, M. C. S. *Adv. Colloid Interface Sci.* **1995**, *58*, 171.
(11) Zielinski, R.; Ikeda, S.; Nomura, H.; Kato, S. *J. Colloid Interface Sci.* **1989**, *129*, 175.
(12) Matsuno, R.; Takami, K.; Ishihara, K. *Langmuir* **2010**, *26*, 13028.
(13) Diaz Garcia, M. E.; Sanz-Medel, A. *Talanta* **1986**, *33*, 255.
(14) Kunieda, H.; Shinoda, K. *J. Phys. Chem.* **1976**, *80*, 246.
(15) Mills, C. O.; Martin, G. H.; Elias, E. *Biochim. Biophys. Acta* **1986**, *876*, 677.
(16) Patist, A.; Bhagwat, B. B.; Penfield, K. W.; Aikens, P.; Shah, D. O. *J. Surfactants Deterg.* **2000**, *3*, 53.
(17) Dar, A. A.; Rather, G. M.; Das, A. R. *J. Phys. Chem. B* **2007**, *111*, 3122.
(18) Domingues, C. C.; Malheiros, S. V. P.; de Paula, E. *Braz. J. Med. Biol. Res.* **2008**, *41*, 758.
(19) Bijma, K.; Engberts, J. B. F. N.; Haandrikman, G.; van Os, N. M.; Blandamer, M. J.; Butt, M. D.; Cullis, P. M. *Langmuir* **1994**, *10*, 2578.
(20) Bhattacharya, S.; Haldar, J. *Langmuir* **2005**, *21*, 5747.
(21) Olofsson, G. *J. Phys. Chem.* **1985**, *89*, 1473.
(22) Kresheck, G. C. *J. Phys. Chem. B* **1998**, *102*, 6596.
(23) Blandamer, M. J.; Cullis, P. M.; Engberts, J. B. F. N. *Pure Appl. Chem.* **1996**, *68*, 1577.
(24) Heerklotz, H.; Epand, R. M. *Biophys. J.* **2001**, *80*, 271.
(25) Hildebrand, A.; Garidel, P.; Neubert, R.; Blume, A. *Langmuir* **2004**, *20*, 320.
(26) Kresheck, G. C. *J. Colloid Interface Sci.* **2006**, *298*, 432.
(27) Paula, S.; Siis, W.; Tuchtenhagen, J.; Blume, A. *J. Phys. Chem.* **1995**, *99*, 11742.
(28) Garidel, P.; Hildebrand, A.; Neubert, R.; Blume, A. *Langmuir* **2000**, *16*, 5267.
(29) Majhi, P. R.; Blume, A. *Langmuir* **2001**, *17*, 3844.
(30) Mehrian, T.; de Keizer, A.; Korteweg, A. J.; Lyklema, J. *Colloids Surf. A: Physicochem. Eng. Asp.* **1993**, *71*, 255.
(31) Nusselder, J. J. H.; Engberts, J. B. F. N. *J. Colloid Interface Sci.* **1992**, *148*, 353.
(32) Kresheck, G. C. *J. Phys. Chem. B* **2009**, *113*, 6732.
(33) Lah, J.; Bešter-Rogač, M.; Perger, T.-N.; Vesnaver, G. *J. Phys. Chem. B* **2006**, *110*, 23279.
(34) Chevallet, M.; Sabtoni, V.; Poinas, A.; Rouquié, D.; Fuchs, A.; Kieffer, S.; Rossignol, M.; Lunardi, J.; Garin, J.; Rabilloud, T. *Electrophoresis* **1998**, *19*, 1901.
(35) Henningsen, R.; Gale, B. L.; Straub, K. M.; De Nagel, D. C. *Proteomics* **2002**, *2*, 1479.
(36) Luche, L.; Santoni, V.; Rabilloud, T. *Proteomics* **2003**, *3*, 249.
(37) Dias, R. S.; Svingen, R.; Gustavsson, B.; Lindman, B.; Miguel, M. G.; Åkerman, B. *Electrophoresis* **2005**, *26*, 2908.
(38) Wiseman, T.; Williston, S.; Brandts, J. F.; Lin, L.-N. *Anal. Biochem.* **1989**, *179*, 131.
(39) Piotto, M.; Saudek, V.; Sklenar, V. *J. Biomol. NMR* **1992**, *2*, 661.
(40) Bax, A.; Davis, D. G. *J. Magn. Reson.* **1985**, *65*, 355.
(41) Bain, A. D.; Burton, I. W. *Concepts Magn. Reson.* **1996**, *8*, 191.
(42) Marion, D.; Wuthrich, K. *Biochem. Biophys. Res. Commun.* **1983**, *113*, 967.

(43) Sklenar, V.; Piotto, M.; Leppik, R.; Saudek, V. *J. Magn. Reson., Ser. A* **1993**, *102*, 241.
(44) Sattler, M.; Maurer, M.; Schleucher, J.; Griesinger, C. *J. Biomol. NMR* **1995**, *5*, 97.
(45) Guinier, A.; Fournet, G. *Small Angle Scattering of X-Rays*; Wiley: New York, 1955.
(46) Svergun, D. I.; Feigin, L. A. *Structure analysis by Small-angle X-ray and Neutron Scattering*; Plenum Press: New York, 1987.
(47) Glatter, O.; Kratky, O. *Small Angle X-ray Scattering*; Academic Press: San Diego, CA, 1982.
(48) Marignan, J.; Basserau, P.; Delord, P. *J. Phys. Chem.* **1986**, *90*, 645.
(49) Barbosa, L. R. S.; Caetano, W.; Itri, R.; Homem-De-Mello, P.; Santiago, P. S.; Tabak, M. *J. Phys. Chem. B* **2006**, *110*, 13086.
(50) Sinibaldi, R.; Ortore, M. G.; Mariani, P. *J. Chem. Phys.* **2007**, *126*, 235101.
(51) Sinibaldi, R.; Ortore, M. G.; Mariani, P. *Eur. Biophys. J.* **2008**, *37*, 673.
(52) Barbosa, L. R. S.; Ortore, M. G.; Spinozzi, F.; Mariani, P.; Bernstorff, S.; Itri, R. *Biophys. J.* **2010**, *98*, 147.
(53) Barbosa, L. R. S.; Rigos, C. F.; Yoneda, J. S.; Itri, R.; Ciancaglini, P. *J. Phys. Chemistry B* **2010**, *114*, 11371.
(54) Press, W. H.; Teukolsky, S. A.; Flannery, B. P. *Numerical Recipes. The Art of Scientific Computing*; Cambridge University Press: Cambridge, U.K., 1994.
(55) Tanford, C. *J. Phys. Chem.* **1972**, *76*, 3020.
(56) Teixeira, C. V.; Itri, R.; Casallanovo, F.; Schreier, S. *Biochim. Biophys. Acta* **2001**, *93*, 1510.
(57) Weers, J. G.; Rathman, J. F.; Axe, F. U.; Crichlow, C. A.; Foland, L. D.; Scheuing, D. R.; Zielske, A. G. *Langmuir* **1991**, *7*, 854.
(58) Graciani, M. M.; Rodríguez, A. M.; Muñoz, M.; Moyá, M. L. *Langmuir* **2005**, *21*, 7161.
(59) Lumry, R.; Rajender, S. *Biopolymers* **1970**, *9*, 1125.
(60) Sugihara, G.; Hisatomi, M. *J. Colloid Interface Sci.* **1999**, *219*, 31.
(61) Gill, S. J.; Wadso, I. *Proc. Natl. Acad. Sci. U.S.A.* **1976**, *73*, 2955.
(62) Priebe, J. P.; Satnami, M. L.; Tondo, D, W.; Souza, B, S.; Priebe, J. M.; Micke, G. A.; Costa, A. C. O.; Fiedler, H. D.; Bunton, C. A.; Nome, F. *J. Phys. Chem. B* **2008**, *112*, 14373.
(63) Ken A. Dill, K. A.; Stigter, D. *Biochemistry* **1988**, *27*, 3446.
(64) Scherer, P. G.; Seelig, J. *EMBO J.* **1987**, *10*, 2915.
(65) Sachs, J.N.; Nanda, H.; Petrache, H. I.; Woolfz, T. B. *Biophys. J.* **2004**, *86*, 187.
(66) Caetano, W.; Barbosa, L. R. S.; Itri, R.; Tabak, M. *J. Colloid Interface Sci.* **2003**, *260*, 414.